Blue-Green Systems

IWA PUBLISHING

Blue-Green Systems Vol 00 No 0, 1 doi: 10.2166/bgs.2023.044

Evaluating the stormwater management model for hydrological simulation of infiltration swales in cold climates

Camillo Bosco [a,*], Elhadi Mohsen Hassan Abdalla [a], Tone Merete Muthanna [b], Knut Alfredsen [b], Britt Rasten[c], Heidi Kjennbakken[d] and Edvard Sivertsen [a]

[a] SINTEF AS, S.P. Andersens vei 3, Trondheim 7031, Norway
[b] Department of Civil and Environmental Engineering, The Norwegian University of Science and Technology, S.P. Andersens vei 5, Trondheim 7031, Norway
[c] Multiconsult Norge AS, Nedre Skøyen vei 2, Oslo 0276, Norway
[d] Norwegian Public Roads Administration, Directorate of public roads, Brynsengfaret 6A, Oslo 0667, Norway
*Corresponding author. E-mail: camillo.bosco@sintef.no

CB, 0000-0002-0710-5505; EMHA, 0000-0002-9871-9034; TMM, 0000-0002-4438-2202; KA, 0000-0002-4076-8351; ES, 0000-0003-1968-170X

ABSTRACT

The Stormwater Management Model (SWMM) is a widely used tool for assessing the hydrological performance of infiltration swales. However, validating the accuracy of SWMM simulation against observed data has been challenging, primarily because well-functioning infiltration swales rarely produce surface runoff, especially over short monitoring periods. This study addresses this challenge by using measured subsurface water storage levels for calibration and validation. The study evaluated three SWMM modules, namely, the snowpack, aquifer, and low-impact development (LID) modules, to simulate subsurface water storage levels of an infiltration swale located in a cold climate region during snow and snow-free periods. Global sensitivity analysis was used to identify influential parameters within these modules. The findings revealed that only a few parameters significantly influenced model outputs. Moreover, the aquifer module outperformed the LID module in simulating subsurface water storage due to limitations in setting the initial saturation of the LID module. Furthermore, simulation accuracy was better during snow-free periods due to challenges in simulating snow dynamics during snow periods with the snowpack module. The calibrated models offer valuable insights into the long-term hydrological performance of infiltration swales, enabling practitioners to identify events that trigger flooding in these systems.

Key words: groundwater monitoring, hydrological modelling, infiltration swale, SWMM

HIGHLIGHTS

- Groundwater data were used to evaluate the long-term performances of infiltration swales.
- Sensitivity analysis identified key parameters in three selected modules in Stormwater Management Model.
- Aquifer and snowpack modules effectively predicted swale hydrological performances.
- Groundwater monitoring reduces uncertainties in soil and snow processes in swales.

1. INTRODUCTION

Infiltration swales are sustainable stormwater infrastructures that convey and infiltrate surface runoff from adjacent roads and connected catchments (Davis *et al.* 2012). They have attracted increasing attention in recent years due to the increased amount of runoff in urban watersheds as a result of climate change and rapid urbanization (Davis *et al.* 2012; Skougaard Kaspersen *et al.* 2017; Sañudo-Fontaneda *et al.* 2020; Bosco *et al.* 2022). Infiltration swales provide other benefits for urban watersheds such as removing sediments and pollutants from surface runoff (Monrabal-Martinez *et al.* 2018; Gavrić *et al.* 2019), reducing the emission of greenhouse gases by capturing carbon, groundwater recharge, and the reduction of soil erosion (Li *et al.* 1998).

The Stormwater Management Model (SWMM) is one of the most commonly used tools for assessing the hydrological performance of sustainable stormwater infrastructure such as infiltration swales, green roofs, and bioretention cells (Rossman 2010). According to the Web of Science database, SWMM has been mentioned in over 1,500 studies in general, and in nearly 500 publications dealing with sustainable stormwater infrastructures,

as of September 2023. Moreover, SWMM has been applied in numerous studies for simulating the hydrological performance of infiltration swales (Hwang & Weng 2015; Peng *et al.* 2020; Bond *et al.* 2021).

For accurate and reliable results of the SWMM model, calibration is required (Alfredo *et al.* 2010; Rosa *et al.* 2015; Peng & Stovin 2017). Rosa *et al.* (2015) tested the performance of an uncalibrated SWMM model in simulating runoff from a catchment with sustainable stormwater infrastructures. They found the model to yield simulation results of catchment outflows with poor agreement with measured values. Hence, they advised to exercise caution when interpreting the results of uncalibrated SWMM models. Typically, sustainable stormwater infrastructures such as green roofs, bioretention cells, and permeable pavements are calibrated using observed drainage outflows as variables for calibration. However, infiltration swales are rarely equipped with drainage pipes, limiting the calibration variables to surface runoff.

Infiltration swales are typically designed with highly porous materials to enhance infiltration and reduce the occurrence of surface runoff and overflooding. Therefore, the occurrence of surface runoff is infrequent in a well-drained infiltration swale. For instance, Sañudo-Fontaneda *et al.* (2020) reported the hydrological performance of infiltration swales over 3.5 years. They found the swale to infiltrate most rainfall events, and only four rainfall events caused surface runoff in swales. Likewise, Davis *et al.* (2012) reported the hydrological performance of four full-scale swales during 52 rainfall events that occurred over a period of 4.5 years. They found half of the events to be infiltrated completely by swales, resulting in no surface runoff. In addition, they reported reduced infiltration volumes for extreme rainfall events yielding surface runoff. It is important to emphasize that such types of events (i.e., extreme events) rarely occur, particularly over short monitoring periods.

The lack of calibration data for infiltration swales can be clearly seen in the literature. Numerous studies have applied SWMM to simulate infiltration swales outflows without prior calibration (see, for instance, Hwang & Weng 2015; Luan *et al.* 2017; Xie *et al.* 2017; Peng *et al.* 2020; Dutta *et al.* 2021, among many others). Only one study was found by the authors to calibrate SWMM models of infiltration swales with measured data (Bond *et al.* 2021), in which surface runoff was used as a variable for calibration. The lack of calibration data for infiltration swales can be addressed in several ways. For instance, artificial rainfall events *in situ* (Hamouz *et al.* 2020) or at the laboratory (Rujner *et al.* 2018) can be used to generate runoff under extreme conditions. Another option is the use of subsurface water storage under the swale as a variable for model calibration. This option can offer a valuable solution when calibrating hydrological models for swales that are monitored over short periods of time, particularly with the lack of extreme rainfall events that can trigger surface runoff. The subsurface water levels can be simulated in SWMM by the aquifer module, which simulates the flow and dynamics of shallow and deep groundwater (Rossman 2010).

The aquifer module of the SWMM model has been evaluated in a few studies at large catchment scales (Wu *et al.* 2008; Pells & Pells 2016; Moore *et al.* 2017), but not in simulating the dynamics of subsurface water levels of sustainable stormwater infrastructures such as infiltration swales. Therefore, there is a need for extensive evaluation of the suitability of the module to simulate sustainable stormwater infrastructures such as infiltration swales. In addition, the performance of the aquifer module needs to be tested in different climates such as in cold climate regions with the presence of snow. Moreover, the results of the aquifer model need to be compared with the results of the low-impact development (LID) module of SWMM, which is commonly used to simulate sustainable stormwater infrastructures in literature. Therefore, the present study attempted to achieve the following objectives:

(i) Evaluating the sensitivity of the parameters of the analysed SWMM modules (i.e., aquifer and LID modules) to determine the most influential parameters affecting the performance in simulating subsurface dynamics.
(ii) Evaluating the accuracy of the analysed SWMM modules in simulating the dynamics of subsurface water levels in snow and snow-free periods.
(iii) Investigating the long-term hydrological performance of infiltration swales using the results of simulation from the calibrated SWMM modules.

The outcomes of the three mentioned objectives can provide support to practitioners when designing and maintaining infiltration swales. In Norway, the stormwater management strategy involves a three-step approach that aims to retain (e.g., infiltrate) small-size rainfall events locally, detain medium-size events, and secure a safe flood path for extreme rainfall events (Lindholm *et al.* 2008). Similar strategies are also implemented in other countries, such as Denmark's three-point approach (Fratini *et al.* 2012). To effectively implement these strategies, a clear

understanding of the performance of stormwater infrastructures (such as LID) is required, especially under different types of rainfall events.

2. MATERIALS AND METHODS

2.1. Case study description

A pilot project on stormwater management, in connection to parts of the road Rv3 in Norway, between Ommangsvollen and Grundset, has been established by Klima 2050, a Norwegian Centre for Research-based Innovation (www.klima2050.no). An infiltration swale (about 700 m long) is installed along a part of the road as a stormwater management solution (Figure A1 in the Supplementary Material) that should infiltrate, treat, detain, and convey stormwater from the road.

Groundwater level data loggers (branded HOBO, type MX2001) are located at different positions along the swale and recorded with a time resolution of 10 min. The sensors are installed by the National Public Roads Administration (NPRA) to provide data that can contribute to the evaluation of the swale's performance. The adopted water level sensors are installed in wells and drilled down to different soil layers. Specifically, PVC pipes inside different wells are perforated at the layers of interest, so groundwater levels are monitored at different depths (Figure A2 in Supplementary Material).

The most central water level sensor along the swale with a depth equal to 2 m was considered for performance assessment of the vegetated swale, given its good representation of the groundwater level for the whole sub-catchment of the swale and since it recorded water levels values for the longest period, from July 2020 to November 2022 (Lillegraven 2021).

A climate station was also installed close to the most upstream section of the considered swale. Registered parameters include precipitation and air temperature. These measurements are collected via NPRA's database whose available values from November 2020 to August 2022 are shown in Figure 1 together with the corresponding groundwater levels recorded at the aforementioned central location.

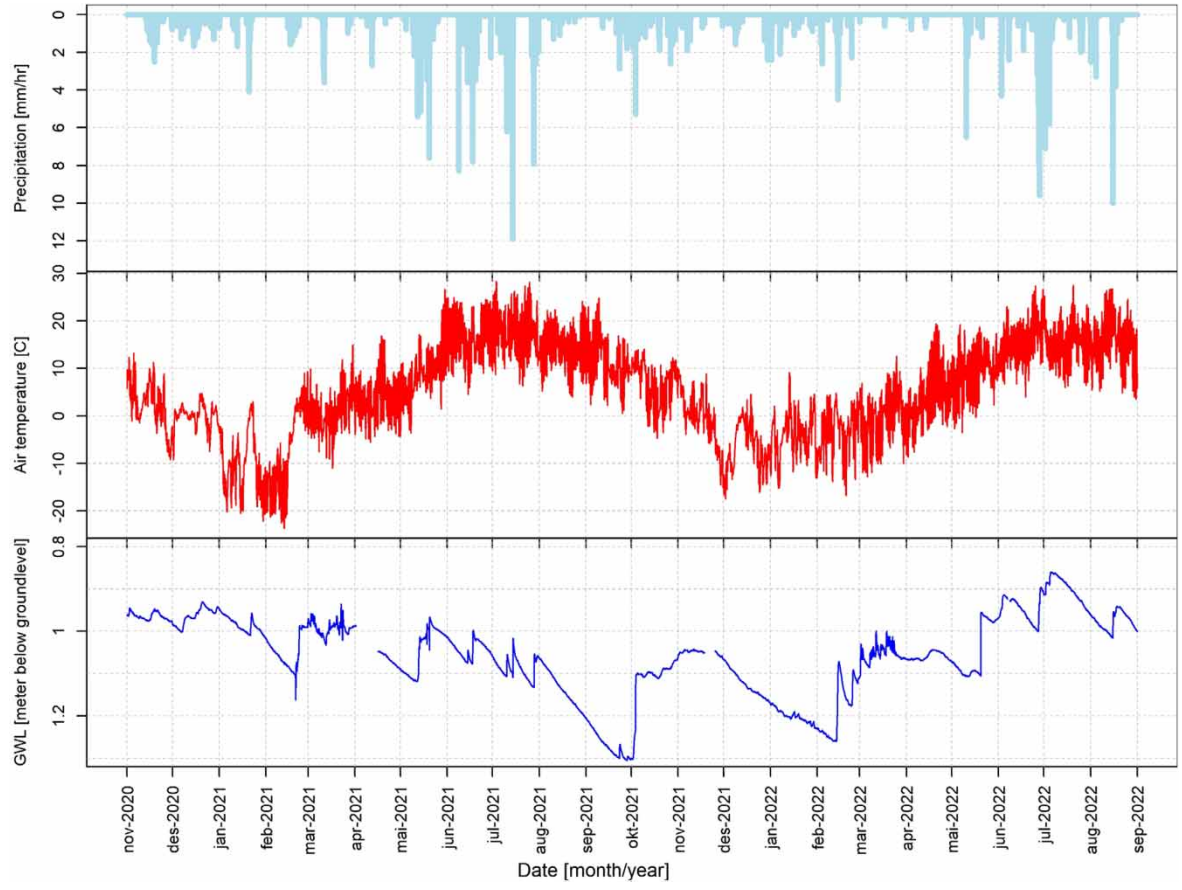

Figure 1 | Observed precipitation, temperatures, and groundwater level values at the weather station and the selected data logger owned by NPRA.

2.2. The stormwater management model

2.2.1. SWMM snowpack module

The snowpack module is a crucial component of SWMM for cold climate regions, which enables the simulation of snowpack processes in urban and rural areas. In the adopted model, the degree-day method was considered, similar to the method presented in the study by Hamouz & Muthanna (2019). The relevant parameters for the degree-day method which needed to be calibrated include the fraction-free water capacity *Cpro*, the site base temperature for snow formation *Tx*, the melting coefficient *Cx* (Rossman 2010), and the antecedent temperature index *ATI* (reflecting to what degree heat transfer within a snow pack during non-melt periods is affected by prior air temperatures), which capture the relationship used in the degree-day method between the amount of snow melting, and the difference between air temperature T and base temperature Ts.

In this study, human-made snow redistribution occurred in the sub-catchment part corresponding to the road, where all the cumulated snow is considered to be moved onto the area of the adjacent vegetated swale, according to the operations performed by the road manager.

2.2.2. SWMM aquifer module

The SWMM aquifer module allows for the simulation of groundwater processes considering the physical properties of the aquifer, including hydraulic conductivity, porosity, and seepage into the deeper soil layers. Interactions with air and water above the level of the ground surface can be modelled through parameters that describe evaporation and lateral surface water recharge, but in the adopted model, those processes were excluded. From the surface, rainwater infiltrates into the upper unsaturated zone according to the Green-Ampt infiltration model. Second, water percolates into the lower saturated zone according to Darcy's equation, given its specific hydraulic conductivity and variation towards the dynamic moisture content, i.e., the conductivity slope. Rainwater is then stored in the lower saturated zone while being depleted into deeper soil layers, according to user-defined equations, depending on the seepage parameter. In the adopted model, the linear default relationship in SWMM between the water table and deep flow depletion was considered (Rossman 2016) (in Figure A3 in Supplementary Material, the definitional sketch from the SWMM's manual of the two-zone groundwater model is depicted together with the representation of flow processes involved).

2.2.3. SWMM LID module

The LID module simulates the hydrological processes of various LID measures such as *vegetative swales* and *bioretention cells* (Rossman 2010). The LID module conceptualizes the *vegetative swale* by one layer (surface layer), which applies the Green-Ampt equation for infiltration and routes excess surface runoff using Manning's formula in a trapezoidal channel (Rossman 2010). However, the *vegetative swale* module does not offer the possibility of modelling the dynamics of subsurface water levels. On the other hand, the *bioretention cell* is conceptualized by four layers in the LID module (i.e., surface, soil, storage, and drain). The infiltration of water in the surface layer to the soil layer can be determined by the Green-Ampt equation. At the storage layer, water either percolates towards the native soil or is routed to the drainage pipe. The routing is determined by an empirical power law equation, based on flow coefficient, exponent, and the offset of the drainage pipe from the bottom of the storage layer. This study used the *bioretention cell* for simulating the dynamics of the subsurface water level of the infiltration swale, neglecting contributions of lateral and horizontal flows.

2.3. Sensitivity of SWMM model parameters

In this study, the Sobol method (Sobol 2001), a global sensitivity analysis technique, was employed to evaluate the sensitivity of parameters in the adopted modules. The *Sensobol* package in R (Puy *et al.* 2022) was used to compute Sobol indices, which measure the impact of individual parameters and their interactions on the overall model variance (Sobol 2001). Although analytical derivation of Sobol indices is possible, the complexity of environmental models often necessitates Monte Carlo integration to approximate their values. To sample model parameters, the Sobol sequence, a quasi-random sampling approach (Sobol 2001), was utilized. This sampling approach generates $N \times (p + 2)$ parameter sets (Puy *et al.* 2022), where p represents the number of model parameters and N denotes the number of samples. In this work, N was set to 5,000, consistent with prior studies (Nossent *et al.* 2011; Brunetti *et al.* 2016). The sensitivity of the model parameters was assessed for the considered modules in snow and snow-free simulation periods. The details of the different parameters

considered in the sensitivity and correlation analyses of the aquifer, LID control, and snowpack modules are reported in Table 1.

2.4. Calibration and validation

The retrieved sensitive parameters of the considered modules were included for model calibration. Calibration was performed using the differential evolution (DE) algorithm (Storn & Price 1997) for both snow and snow-free periods. DE is a population-based algorithm that searches for optimal parameter sets within user-defined ranges (upper and lower limits in Table 1). DE begins by selecting an initial population of parameter sets and evaluating their goodness of fit using a defined objective function.

The algorithm then evolves each population to the next by improving or maintaining the objective function value of each parameter set, until the maximum number of populations is reached (200 in this study). The optimal parameter set in the final population is selected as the optimal one. In this study, the Nash–Sutcliffe efficiency (NSE) was used as the objective function, and the size of the population was chosen as 10 times the number of parameters. The calibration and validation were performed for two distinct simulation periods, respectively, from 1 November 2020 to 1 May 2021 and from 1 November 2021 to 1 May 2022 for snow periods and from

Table 1 | Parameters of the SWMM modules

Module	Layer	Parameter	Symbol	Unit	Lower limit[a]	Upper limit[a]	Fixed/ optimal value[b]
Snowpack		Melting factor	*Cx*	mm/°C	0	1	0.05
		Base temperature for melting	*Tx*	°C	−3	3	−1.67
		Free liquid water in the snowpack	*cpro*	–[d]	0	1	0.423
		Threshold temperature between rainfall and snowfall	*Ts*	°C	−3	3	−1.07
		Antecedent temperature index weight	*ATI*	–[d]	0	1	0.38
		Negative melt ratio	*N.melt.ratio*	–[d]	0	1	0.074
Catchment + aquifer	Surface (catchment)	Suction head	*sh*	mm	0	100	37
		Saturated hydraulic conductivity	*Ksat_sw*	mm/hr	0.1	1,000	750
		Initial soil moisture deficit	*IMD*	–[d]	0.09	1	0.52
	Aquifer	Porosity	*POR*	–[d]	0.1	0.9	0.89
		Wilting point	*WP*	–[d]			0
		Field capacity	*FC*	–[d]			0.01
		Saturated hydraulic conductivity	*Ksat_gw*	mm/hr	0.1	1,000	833.9
		Conductivity slope	*k_slope*	–[d]	0	100	8.47
		Tension slope	*Tslope*	mm	0	100	23
		GW percolation rate (seepage)	*Seep*	mm/hr	0	1	0.331–0.17[c]
LID (bioretention cell)	Surface	Manning	*mann*	–[d]	0.001	0.3	0.1
	Soil	Thickness		M			0.8
		Porosity	*Por*	–[d]	0.1	0.6	0.29
		Field capacity	*FC*	–[d]			0.01
		Wilting point	*WP*	–[d]			0
		Conductivity	*ksat*	mm/hr	0.1	1,000	983
		Conductivity slope	*k_slope*	–[d]	0.1	100	48.91
		Suction head	*Sh*	mm	0	100	3.5
	Storage	Void fraction	*Void*	–[d]	0.01	0.9	0.75
		Thickness		M			2.2
	Drain	Flow coefficient	*kcoeff*	–[d]	0	1	0.011
		Flow exponent	*expon*	–[d]	0	3	0.33

[a]Based on the SWMM manual, and relevant studies in the literature.
[b]The results of model calibration.
[c]Optimal values of seepage for the snow-free period (0.331) and the snow period (0.17).
[d]Unitless (ratio).

1 November 2020 to 1 May 2021 and from 1 November 2021 to 1 May 2022 for snow-free periods. The separation of the two periods was based on the temperature values reported in Figure 1, with snow-free periods having weekly temperatures steadily above 0 °C.

2.5. Scenarios for long-term performances of the swale

The calibrated model was adopted to generate long-term time series (2010–2020) of surface runoff and subsurface water levels, utilizing precipitation and temperature measurements of two Norwegian cities, namely, Hamar and Bergen (in SM). Flow duration curves (FDCs) related to surface runoff were considered to analyse the long-term hydrological performances of the considered infiltration swale. The derivation of FDC was carried out in a similar way as in previous studies (Abdalla *et al.* 2021; Abdalla *et al.* 2022b).

Precipitation and temperature data were collected, checked, and corrected by the Norwegian Meteorological Institute (MET) (Lutz *et al.* 2020). The two cities have distinct climate conditions, with Bergen receiving an average high annual precipitation equal to 3,110 mm and Hamar receiving only 650 mm. In addition, the two cities belong to different climatic classes based on the Köppen–Geiger system, with Bergen classified as a temperate oceanic climate (Cfb) and Hamar classified as a warm-summer humid continental climate (Dfb). It is worth noting that the pilot swale examined in this study is located alongside a main road close to Hamar city (as shown in Figure A4 in Supplementary Material).

3. RESULTS AND DISCUSSION

3.1. Sensitivity and correlations for the considered modules

Figure 2 presents the results of the Sobol sensitivity analysis which aims at evaluating the importance of each parameter in the different adopted modules, with and without snowpack simulations. As shown in Figure 2, the most sensitive parameters of the aquifer module are *seepage (seep)*, *porosity (por)*, and *conductivity slope (Kslope)*. However, *hydraulic conductivity* (*Ksat_gw*) was also included in the calibration process, especially given its correlation with the *conductivity slope* (*Kslope*) (see Figure A4 in Supplementary Material for details).

In the adopted LID module, the most important parameters relate to the drainage layer characteristics, namely, the *offset* above the bottom of the storage layer, and the parameters *orifice coefficient (kcoeff)* and *orifice exponent* (*expon)*, which describe together the orifice law of the mentioned storage, respectively, as coefficient and exponent. The sensitivity of these two latter parameters was reported by many studies that evaluated different LID modules of SWMM such as permeable pavement (Abdalla *et al.* 2021) and bioretention cell (Hernes *et al.* 2020). *Porosity*, *hydraulic conductivity*, and *conductivity slope* were also included in the calibration process of the adopted LID module to allow a comparison with the corresponding optimal values obtained for the aquifer module. Concerning snowpack modelling, as shown in Figure 2, righthand subplots, the sensitive parameters are *Cx*, *Cpro*, and *Tx*, as also found in other studies (Hamouz & Muthanna 2019); however, *Ts*, *ATI*, and *Negative Melt Ratio* were also included in the calibration process.

The results revealed strong correlations among the most sensitive parameters of each module (Figure A5 in Supplementary Material presents the correlations between different parameters within each module). For example, in the aquifer module, a significant negative correlation was found between the *seep* parameter and both *Por* and *k_slope* during both snow and snow-free periods. As a result of these high correlations, a large difference can be noted between the first-order and total Sobol indices (Figure 2), indicating that the sensitivity of some parameters, such as *Por*, is primarily driven by their correlation with other model parameters. This results in equifinality, in which different values of model parameters lead to the same model outcome (Beven 1993). It can be noted that some studies attempted to address the issue of equifinality by utilizing multi-objective optimization methods (Fowler *et al.* 2016; Saavedra *et al.* 2022; Abdalla *et al.* 2023) and by utilizing multiple data (Seibert 2000; Parajka *et al.* 2009; Abdalla *et al.* 2022a) to reduce equifinality and enhance transferability of the hydrological models.

The results of the sensitivity analysis showed that only a few parameters control the dynamics of the groundwater levels for the SWMM modules and most of the parameters were found to be insensitive. This could potentially reduce the time and computation costs needed to parameterize the considered SWMM modules for future studies.

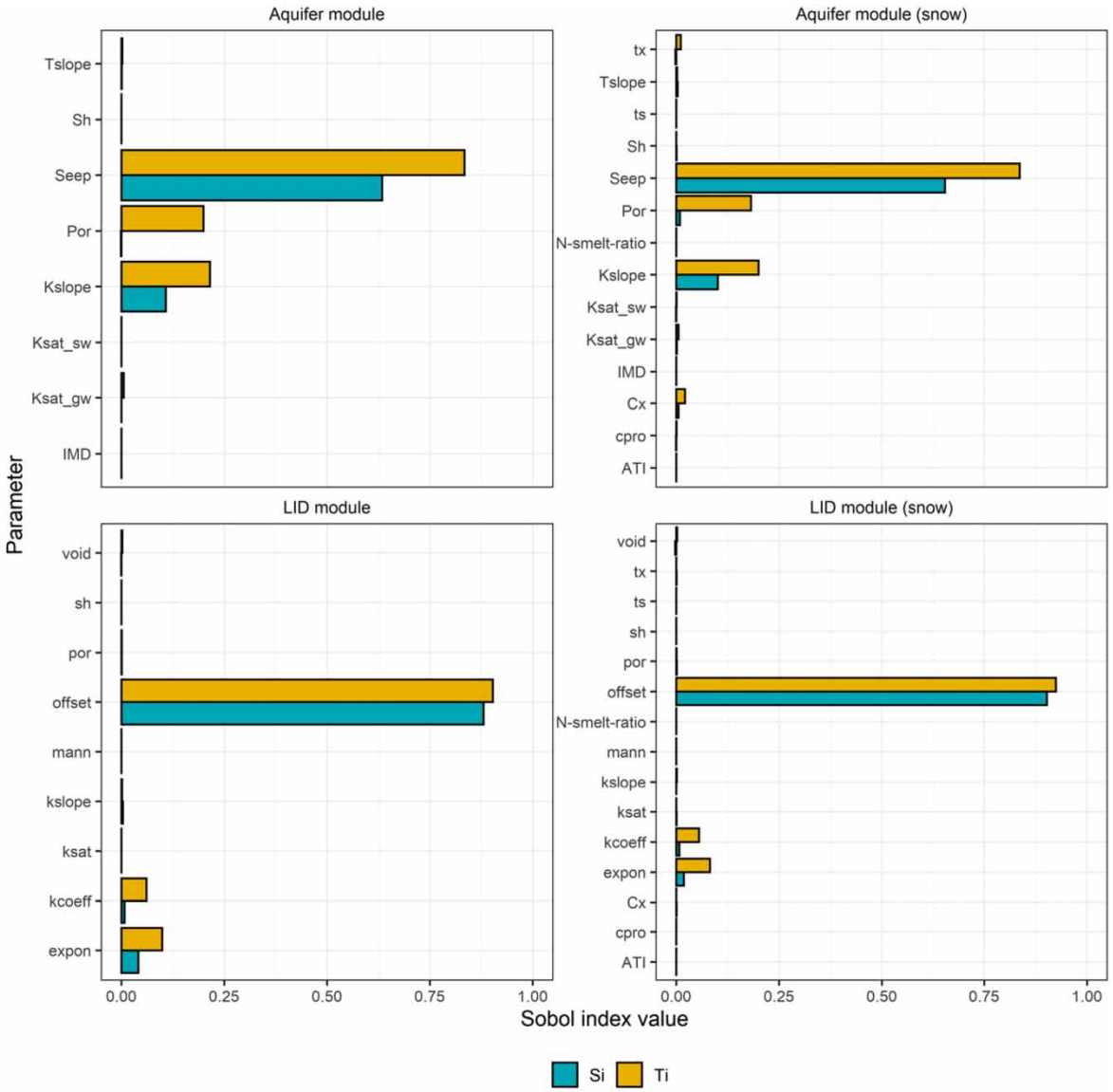

Figure 2 | First-order (Si) and total sensitivity indexes (Ti) for the aquifer and LID modules with and without snowpack modelling.

3.2. Calibration and validation of the considered modules

As described in the previous section, results from calibration and validation were evaluated separately for periods with and without snowpack formation. The results of model calibration are presented in Table 1. The optimization algorithm yielded similar results for most of the parameters between snow and snow-free periods. However, the *seepage* parameter for the aquifer and the LID modules differed significantly between snow and snow-free periods, as reported in Table 1. The optimal value for the *seepage* parameter was almost half during snow periods compared to the optimal value obtained for snow-free periods.

This difference in the values of the *seepage* parameter can be attributed to the changing properties of the deeper native soil with different temperature regimes. The relationship between temperature and infiltration rate has been investigated in the literature. For example, Jaynes (1990) conducted a study on an agricultural field in which the infiltration rate, water viscosity, and temperature were monitored for a period of 5 days. The author reported that changes in water viscosity due to temperature had a significant impact on the infiltration rate. Similarly, Braga *et al.* (2007) investigated the effect of temperature on infiltration rates in infiltration swales. Their results showed a 56% increase in infiltration rates during the warm period compared to the cold period. Balstad *et al.* (2018) applied the modified Phillip–Dunne Infiltrometer method to monitor the infiltration capacity of a

rain garden in Norway. They found the saturated hydraulic conductivity to vary between 1 cm/hr during summer periods to 0.05 cm/hr in winter, resulting in a 75% reduction in the infiltration volume in winter, compared to summer periods.

The calibration yielded different values for the parameters with the same name between the aquifer and LID modules such as *ksat* and *k_slope*. This is referred to by Beven (2010) as *parameters' commensurability* in which parameter values are not independent of the model structure used, resulting in different values for different model structures. This can also be linked to the equifinality issue, as discussed earlier, resulting in an unrealistic combination of parameter sets that are difficult to interpret and compare with other cases and model structures. Groundwater levels below the surface of the considered vegetated swale for snow-free periods are shown in Figure 3 for both the aquifer module and the adopted LID module.

Results obtained by adopting the aquifer module outperformed the results from the LID module. The initial poor match between observed groundwater levels and corresponding levels calculated through the LID module is mainly due to an issue linked with the settings of initial saturation which, in SWMM, must be equal in the soil and the storage layers. This causes an immediate percolation in the model from the soil to the storage, resulting in a calculated level with a significantly different value than the observed actual value. Iterations may be performed to find a good initial match; however, associated improvements in the overall results for the whole simulation were proven to be negligible. Given the better fit of the model implementing the bioretention cell module after 2 weeks from the starting day of the simulation, future studies can attempt to adopt an initial warm-up time-window to improve the results on the actual investigated period. In general, the performances

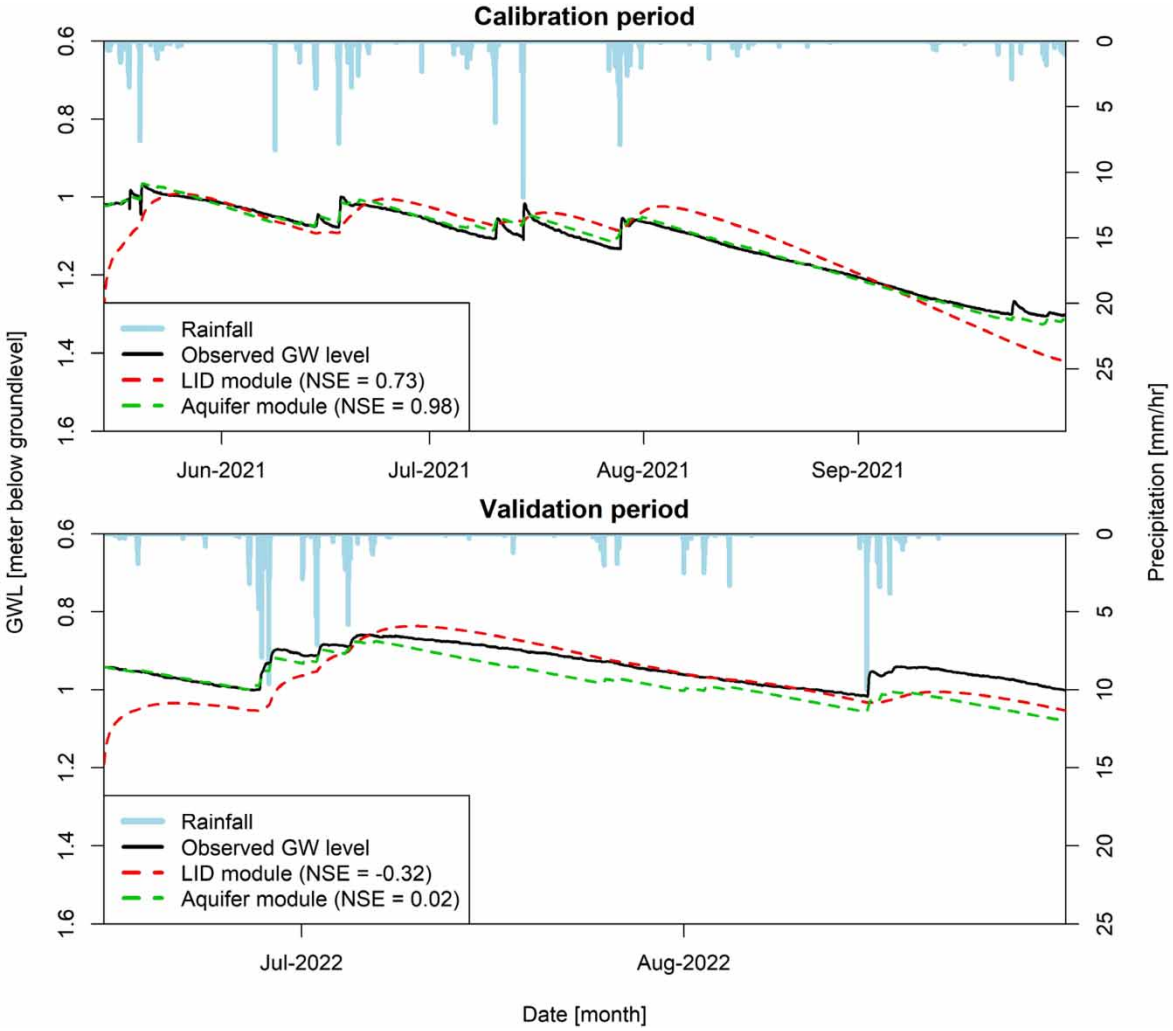

Figure 3 | Comparison between observed and simulated groundwater levels from the calibrated models using either the aquifer or the LID module during periods without snowpack formation.

of the different models in terms of NSE decline from calibration to validation. This might be due to different reasons, such as overfitting of the calibration data or stabilization of soil conditions of the swale. During the calibration period, the variations of the groundwater level were significantly higher than what was observed during the validation period, leading to lower NSE values in the latter case. Moreover, on the one hand, although sensitivity analysis allowed us to single out the most important parameters for tuning the models, the selection might have been insufficient, leading to an overfitting of the models on the calibration dataset which prevents the models from generalizing on different datasets. On the other hand, it should be noted that the installation of the considered swale was performed in 2020 when the adopted data started to be collected; therefore, it is rather likely that transitory soil settings might occur towards a stable condition, at least for the first few years of the infrastructure's life.

The optimal *porosity* value adopted in the calibrated models corresponds to the upper limit of the explored range of values. In fact, the filling process is highly affected by the presence of the wide road subbase course made of high-porosity gravel-type soil, acting similarly as a storage tank, given its large volume compared with the surface of the considered vegetated swale. However, simulation results were also obtained by constraining the *porosity* value to 0.45, closer to the expected value for the type of soil below the surface of the considered swale. As expected, the higher porosity value generated overall better results in terms of NSE, with the lower porosity value producing the effect of neglecting the dynamics of higher frequency (a comparison between the results from the models adopting the two different *porosity* values is depicted in Figure A6 in Supplementary Material).

Groundwater levels below the surface of the considered vegetated swale for periods characterized by snowpack formation and snow melting are depicted in Figure 4 for the aquifer module and the adopted LID control.

Considering the results in Figure 4, results obtained through the aquifer module showed better performances in capturing the dynamics of the observed groundwater levels also for colder periods, characterized by snowpack formation and snow melting. In this case, the errors between calculated and observed groundwater levels in the validation period are generally higher than the ones reported for snow-free periods, as measured also by the NSE scores reported in Figures 3 and 4. In addition to the overfitting of the calibration dataset and the stabilization of soil conditions, the uncertainty about the operations performed by the road manager to cope with snow (such as the time of removal or the adopted frequency for adding salt on the road surface, which enhances snow melting (Koefod *et al.* 2015)) or additional factors for snow redistribution (also dependent on wind or the vehicular traffic) make it challenging to model snow melting processes, leading to larger errors of the validation dataset during spring, as depicted in Figure 4. Moreover, native soil clogging phenomena have been modelled through the *seepage* parameter either with a high or a low value because of the current modelling capabilities of SWMM for snow-free and snow periods, respectively. However, a variable value between the adopted extremes for *seepage* is likely to be closer to reality, especially during snow melting.

3.3. Hydrological performances based on long-term simulation

The long-term simulations were performed adopting the model with the combination of the snowpack module and the aquifer module since the latter showed better results than the considered LID control. As mentioned in Section 3.2, the only parameter which showed significantly different values among the snow and snow-free periods was the *seepage* parameter, which resulted to be almost half during the snow period, compared to the optimal value obtained for the snow-free period. Due to this parameter's sensitivity, three values of the *seepage* parameter were selected to run continuous simulations, namely, the optimal values obtained for snow-free periods, snow periods, and their average.

The simulations considering about 10 years of data from the Hamar and Bergen weather stations, concerning the daily precipitations and daily average temperatures, are shown in Figure 5.

The bandwidth depicted in Figure 5(a) concerning groundwater levels in Hamar expresses the level of uncertainty associated with *seepage*, varying from lower levels for high *seepage* in warmer periods and higher levels for low *seepage* in colder periods. Specifically, the band indicates the range of simulated groundwater levels obtained by varying the value of *seepage* between its maximum and minimum, corresponding to the calibrated values obtained, respectively, for snow-free and snow periods. The climate conditions in Hamar during the last decade produced no surface runoff; therefore, entire rainwater would have been infiltrated into the ground, keeping for most of the time a groundwater depth between 1 and 2 m below the surface of the infiltration swale.

The bandwidth depicted for Bergen in Figure 5(b) concerning groundwater levels shows a lower level of uncertainty associated with the seepage values, in comparison with results shown in Figure 5(a) because, with Bergen

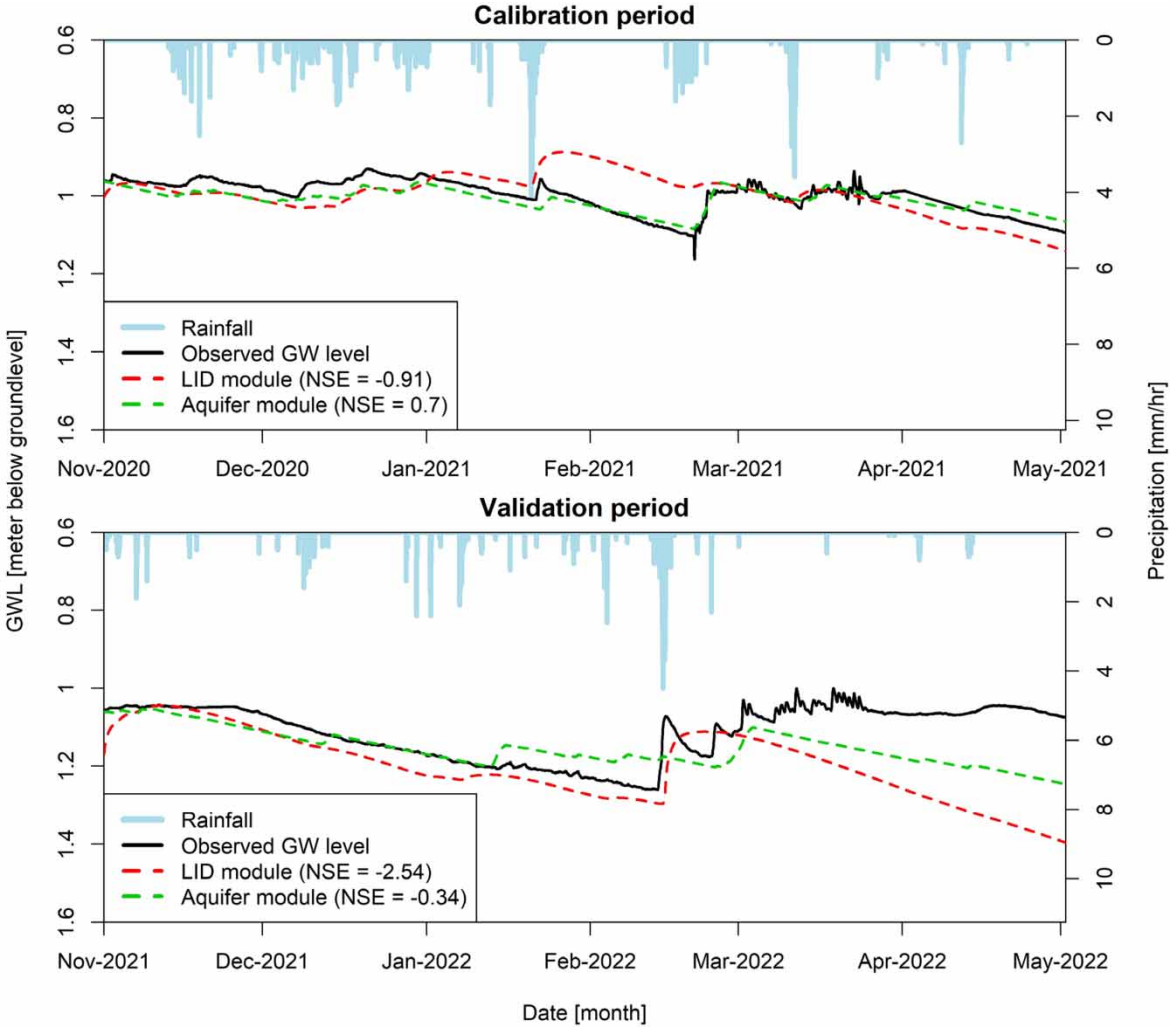

Figure 4 | Comparison between observed and simulated groundwater levels from the calibrated models using either the aquifer or the LID module during periods with snowpack formation.

climate conditions, the considered infiltration swale often reaches full saturation; therefore, the *seepage* values directly affect surface runoff rather than impacting directly on the status of fully saturated soil.

The climate conditions in Bergen during the considered decade produced several events with surface runoff, especially in colder periods. In fact, groundwater levels are generally lower during warmer periods because of lower average precipitations and no contributions of snow melting, as well as a higher value of *seepage*.

The groundwater storage is affected by the total amount of infiltrated rainwater rather than maximum precipitations which have similar values in Hamar and Bergen (Abdalla *et al.* 2022b). Moreover, the modelled infiltration capacity was shown to not be a determining factor in triggering surface runoff since such a case occurred only as a direct consequence of groundwater saturation (Figure A7 in Supplementary Material for details on the FDC related to the surface runoff in Bergen climate conditions).

Yang *et al.* (2015) differentiated between two types of surface runoff in green roofs: saturation-excess runoff (i.e., due to the saturation of green roof layers) and infiltration-excess runoff which occurs when the precipitation intensity exceeds the infiltration capacity of the surface soil. In this study, only the former runoff type was considered due to the high infiltration capacity of the surface layer as the clogging of the surface layer is negligible in the first years of operation, compared to the involved inflow. However, clogging of the surface layer could reduce the infiltration capacity leading to increasing occurrences of infiltration excess runoff in the future. To assess the maximum level corresponding to the saturation excess runoff, HEC-RAS software (Brunner 1995) was used to model hydraulic behaviour in the channel, consisting of the swale and the surrounding catchment, including part of the road. The maximum value reached for a few minutes during the 10-year simulated period was

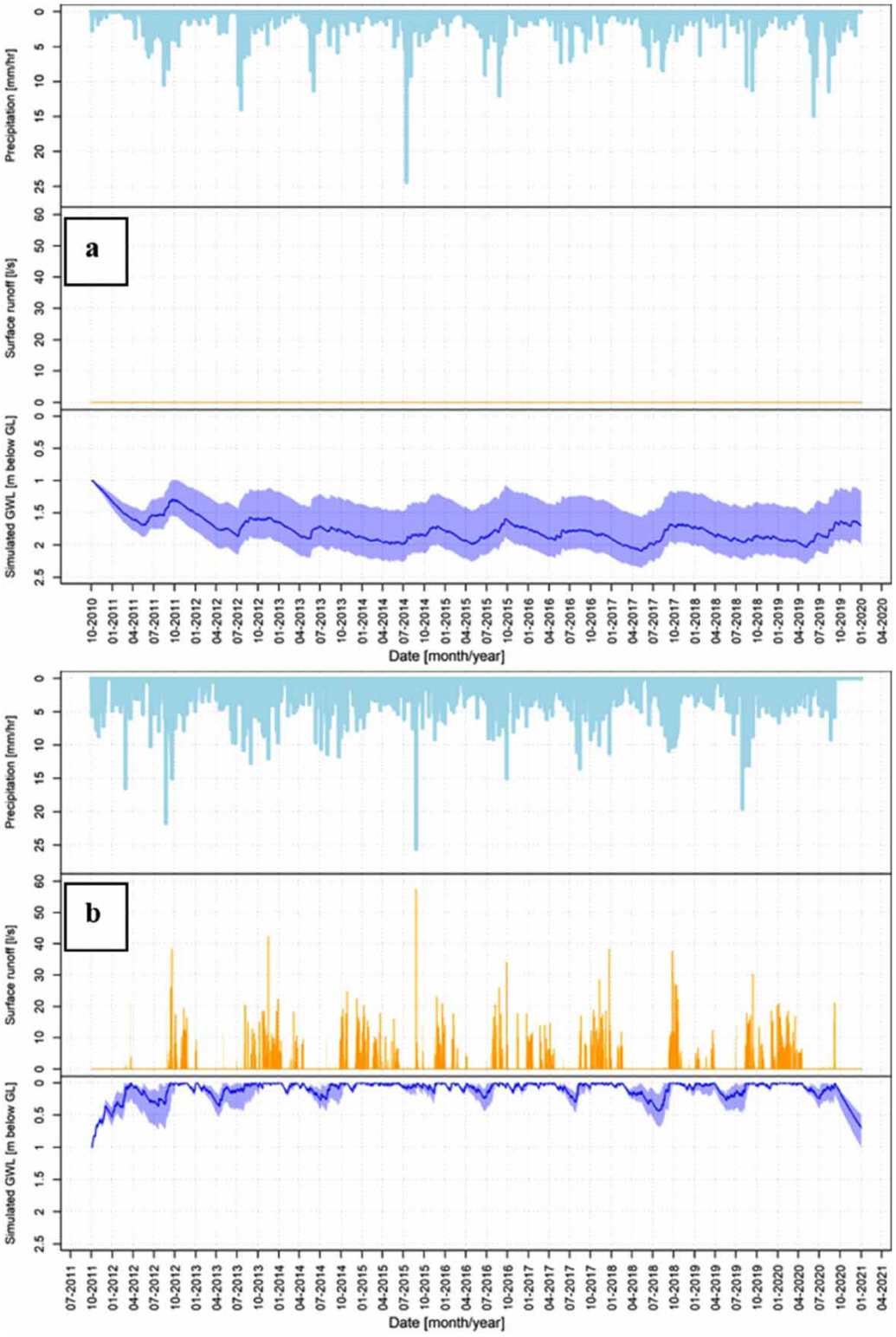

Figure 5 | Long-term time series of Hamar (a) and Bergen (b) precipitation, surface runoff, and groundwater levels simulated through the model with aquifer and snowpack modules considering three different values for seepage.

below 70 L/s and was shown to be safely below the capacity of the swale channel. Details of the HEC-RAS model are not presented in this work; but as a main finding related to this study, hydraulic sufficiency of the swale channel has been verified considering that input discharges the maximum surface runoff obtained, with the aforementioned analysis, while assuming conditions of impermeable channel, given the status of groundwater saturation for the infiltration swale.

4. CONCLUSIONS

In this article, a novel approach was adopted to evaluate the hydrological performances of infiltration swales in cold climates, taking advantage of the continuous measurements of the groundwater level observed in a pilot project in Klima 2050, located along the Norwegian Rv3 road. Overall results of the study shed light on the need for continuous monitoring of groundwater levels in infiltration swales to improve the hydrological modelling of such an infrastructure.

A sensitivity analysis was performed to select the most important parameters of three selected modules in SWMM, namely, aquifer, bioretention cells, and snowpack modules. The calibrated model adopting the aquifer module showed a better agreement with the observations than the model with bioretention cells, mostly because of a limitation in SWMM related to the fact that the initial saturation of the bioretention cells' soil and storage layers cannot be differentiated. The calibrated parameters of the snowpack module showed to be effective in providing a good fit between the model and the observations, especially when coupled with the aquifer module during periods when the temperature was significantly below 0 °C. Snow melting periods during spring were well captured by the model concerning the calibration period, while the dynamics was poorly captured within the validation period, because of several uncertainties, such as the road manager operations for snow management or the actual value of the *seepage* used to model the flow to the deeper native soil. In fact, native soil clogging during freezing months has been modelled by adopting a lower fixed *seepage* value for snow periods compared to the fixed value adopted for snow-free periods. However, intermediate values between the two extremes are likely to be closer to reality, especially during snow melting. Moreover, stable soil conditions have not yet reached in the considered swale since its recent installation; therefore, this could have a large impact on the results of the validation period, related to data recorded 1 year later than the data used for the calibration period.

The combination of the aquifer and snowpack modules was used for 10-year simulations, considering the extreme adopted seepage values and their average. The climate conditions of Hamar and Bergen were taken into account to explore the long-term hydrological performances for the analysed structure of the infiltration swale, resulting in events of surface runoff only in Bergen for its higher total precipitation, assuming similar values of soil properties. Nevertheless, flooding conditions were proven to be always prevented in the analysis because of the large hydraulic capacity of the swale channel compared to the calculated maximum surface runoff. However, monitoring is ongoing, and additional data on the performance of swales will improve the reliability of the model, given the recent construction of the considered infrastructure and its probable transition to stable conditions over the next few years. In the future, additional measurements of groundwater levels and soil properties (e.g., infiltration, percolation, seepage parameters) are planned and will represent desirable data to improve the model performances and advance from the study presented here.

FDCs that are derived from long-term simulations can offer a robust approach for investigating the hydrological performance of LID measures in different types of rainfall events. In addition, monitored groundwater levels present an alternative dataset for evaluating the performance of infiltration swales for low- and medium-size rainfall events. As shown in this study, monitored groundwater levels can be used for calibrating hydrological models of infiltration swales to evaluate their long-term performance using FDCs, preferably accounting for climate change scenarios. It is worth noting that runoff events might have large flooding consequences, especially if rainwater is collected from a basin with a larger extension than the one considered in the present work, mostly consisting of only the infiltration swale itself and the adjacent road.

FUNDING

The work reported in this paper has received funding from the Klima 2050 project, supported by the Norges Forskningsråd and the project partners (Grant no. SFI Klima2050 (237859/030)).

CREDIT AUTHORSHIP CONTRIBUTION STATEMENT

Camillo Bosco: conceptualization, investigation, methodology, formal analysis, data curation, software, validation, visualization, writing – original draft preparation, and writing – review & editing. Elhadi Mohsen Hassan Abdalla: conceptualization, investigation, methodology, formal analysis, software, validation, visualization, writing – original draft preparation, and writing – review & editing. Tone Muthanna: supervision and writing – review & editing. Knut Alfredsen: supervision, resources, and writing – review & editing. Britt

Rasten: funding acquisition, resources, and writing – review & editing. Heidi Kjennbakken: funding acquisition, resources, and writing – review & editing. Edvard Sivertsen: funding acquisition, resources, project administration, conceptualization, methodology, supervision, visualization, and writing – review & editing.

DATA AVAILABILITY STATEMENT

All relevant data are included in the paper or its Supplementary Information.

CONFLICT OF INTEREST

The authors declare there is no conflict.

REFERENCES

Abdalla, E. M. H., Selseth, I., Muthanna, T. M., Helness, H., Alfredsen, K., Gaarden, T. & Sivertsen, E. 2021 Hydrological performance of lined permeable pavements in Norway. *Blue-Green Systems* **3** (1), 107–118. https://doi.org/10.2166/bgs.2021.009.

Abdalla, E. M. H., Alfredsen, K. & Merete Muthanna, T. 2022a Towards improving the calibration practice of conceptual hydrological models of extensive green roofs. *Journal of Hydrology* **607**, 127548. https://doi.org/10.1016/j.jhydrol.2022.127548.

Abdalla, E. M. H., Muthanna, T. M., Alfredsen, K. & Sivertsen, E. 2022b Towards improving the hydrologic design of permeable pavements. *Blue-Green Systems* **4** (2), 197–212. https://doi.org/10.2166/bgs.2022.004.

Abdalla, E. M. H., Alfredsen, K. & Muthanna, T. M. 2023 On the use of multi-objective optimization for multi-site calibration of extensive green roofs. *Journal of Environmental Management* **326**, 116716. https://doi.org/10.1016/j.jenvman.2022.116716.

Alfredo, K., Montalto, F. & Goldstein, A. 2010 Observed and modeled performances of prototype green roof test plots subjected to simulated low- and high-intensity precipitations in a laboratory experiment. *Journal of Hydrologic Engineering* **15** (6), 444–457. https://doi.org/10.1061/(ASCE)HE.1943-5584.0000135.

Balstad, A. S. N., Lohne, J. & Muthanna, T. M. 2018 *Seasonal Variations in Infiltration in Cold Climate Raingardens – A Case Study from Norway*.

Beven, K. 1993 Prophecy, reality and uncertainty in distributed hydrological modelling. *Advances in Water Resources* **16** (1), 41–51. https://doi.org/10.1016/0309-1708(93)90028-E.

Beven, K. 2010 *Environmental Modelling: An Uncertain Future?* CRC Press.

Bond, J., Batchabani, E., Fuamba, M., Courchesne, D. & Trudel, G. 2021 Modeling a bioretention basin and vegetated swale with a trapezoidal cross section using SWMM LID controls. *Journal of Water Management Modeling*. https://doi.org/10.14796/JWMM.C474.

Bosco, C., Raspati, G. S., Tefera, K., Rishovd, H. & Ugarelli, R. 2022 Protection of water distribution networks against cyber and physical threats: The STOP-IT approach demonstrated in a case study. *Water* **14** (23), 3895. https://doi.org/10.3390/w14233895.

Braga, A., Horst, M. & Traver, R. G. 2007 Temperature effects on the infiltration rate through an infiltration basin BMP. *Journal of Irrigation and Drainage Engineering* **133** (6), 593–601. https://doi.org/10.1061/(ASCE)0733-9437(2007)133:6(593).

Brunetti, G., Šimůnek, J. & Piro, P. 2016 A comprehensive numerical analysis of the hydraulic behavior of a permeable pavement. *Journal of Hydrology* **540**, 1146–1161. https://doi.org/10.1016/j.jhydrol.2016.07.030.

Brunner, G. W. 1995 *HEC-RAS River Analysis System. Hydraulic Reference Manual. Version 1.0*. Hydrologic Engineering Center.

Davis, A. P., Stagge, J. H., Jamil, E. & Kim, H. 2012 Hydraulic performance of grass swales for managing highway runoff. *Water Research* **46** (20), 6775–6786. https://doi.org/10.1016/j.watres.2011.10.017.

Dutta, A., Torres, A. S. & Vojinovic, Z. 2021 Evaluation of pollutant removal efficiency by small-scale nature-based solutions focusing on bio-retention cells, vegetative swale and porous pavement. *Water* **13** (17), 2361. https://doi.org/10.3390/w13172361.

Fowler, K. J. A., Peel, M. C., Western, A. W., Zhang, L. & Peterson, T. J. 2016 Simulating runoff under changing climatic conditions: Revisiting an apparent deficiency of conceptual rainfall-runoff models. *Water Resources Research* **52** (3), 1820–1846. https://doi.org/10.1002/2015WR018068.

Fratini, C. F., Geldof, G. D., Kluck, J. & Mikkelsen, P. S. 2012 Three points approach (3PA) for urban flood risk management: A tool to support climate change adaptation through transdisciplinarity and multifunctionality. *Urban Water Journal* **9** (5), 317–331. https://doi.org/10.1080/1573062X.2012.668913.

Gavrić, S., Leonhardt, G., Marsalek, J. & Viklander, M. 2019 Processes improving urban stormwater quality in grass swales and filter strips: A review of research findings. *Science of the Total Environment* **669**, 431–447. https://doi.org/10.1016/j.scitotenv.2019.03.072.

Hamouz, V. & Muthanna, T. M. 2019 Hydrological modelling of green and grey roofs in cold climate with the SWMM model. *Journal of Environmental Management* **249**, 109350. https://doi.org/10.1016/j.jenvman.2019.109350.

Hamouz, V., Pons, V., Sivertsen, E., Raspati, G. S., Bertrand-Krajewski, J.-L. & Muthanna, T. M. 2020 Detention-based green roofs for stormwater management under extreme precipitation due to climate change. *Blue-Green Systems* **2** (1), 250–266. https://doi.org/10.2166/bgs.2020.101.

Hernes, R. R., Gragne, A. S., Abdalla, E. M. H., Braskerud, B. C., Alfredsen, K. & Muthanna, T. M. 2020 Assessing the effects of four SUDS scenarios on combined sewer overflows in Oslo, Norway: Evaluating the low-impact development module of the Mike Urban model. *Hydrology Research* **51** (6), 1437–1454. https://doi.org/10.2166/nh.2020.070.

Hwang, C.-C. & Weng, C.-H. 2015 Effects of rainfall patterns on highway runoff pollution and its control: Highway runoff pollution and its control. *Water and Environment Journal* **29** (2), 214–220. https://doi.org/10.1111/wej.12109.

Jaynes, D. B. 1990 Temperature variations effect on field-measured infiltration. *Soil Science Society of America Journal* **54** (2), 305–312. https://doi.org/10.2136/sssaj1990.03615995005400020002x.

Koefod, S., Mackenzie, R. & Adkins, J. 2015 Effect of prewetting brines on the ice-melting rate of salt at very cold temperatures. *Transportation Research Record: Journal of the Transportation Research Board* **2482** (1), 67–73. https://doi.org/10.3141/2482-09.

Li, J., Orland, R. & Hogenbirk, T. 1998 Environmental road and lot drainage designs: Alternatives to the curb–gutter–sewer system. **25**.

Lillegraven, M. G. 2021 *Hydrological Modelling of Infiltration Swale and Local Ungauged Catchment*. *Master Thesis*, Norwegian University of Science and Technology (NTNU). Available from: https://ntnuopen.ntnu.no/ntnu-xmlui/handle/11250/2787926.

Lindholm, O., Endresen, S., Thorolfsson, S., Sægrov, S., Jakobsen, G. & Aaby, L. 2008 *Veiledning i klimatilpasset overvannshåndtering (Guidance on Climate Adapted Stormwater Management) (162)*. Norsk Vann.

Luan, Q., Fu, X., Song, C., Wang, H., Liu, J. & Wang, Y. 2017 Runoff effect evaluation of LID through SWMM in typical mountainous, low-lying urban areas: A case study in China. *Water* **9** (6), 439. https://doi.org/10.3390/w9060439.

Lutz, J., Grinde, L. & Dyrrdal, A. V. 2020 Estimating rainfall design values for the city of Oslo, Norway – Comparison of methods and quantification of uncertainty. *Water* **12** (6), 1735. https://doi.org/10.3390/w12061735.

Monrabal-Martinez, C., Aberle, J., Muthanna, T. M. & Orts-Zamorano, M. 2018 Hydrological benefits of filtering swales for metal removal. *Water Research* **145**, 509–517. https://doi.org/10.1016/j.watres.2018.08.051.

Moore, M. F., Vasconcelos, J. G. & Zech, W. C. 2017 Modeling highway stormwater runoff and groundwater table variations with SWMM and GSSHA. *Journal of Hydrologic Engineering* **22** (8), 04017025. https://doi.org/10.1061/(ASCE)HE.1943-5584.0001537.

Nossent, J., Elsen, P. & Bauwens, W. 2011 Sobol' sensitivity analysis of a complex environmental model. *Environmental Modelling & Software* **26** (12), 1515–1525. https://doi.org/10.1016/j.envsoft.2011.08.010.

Parajka, J., Naeimi, V., Blöschl, G. & Komma, J. 2009 Matching ERS scatterometer based soil moisture patterns with simulations of a conceptual dual layer hydrologic model over Austria. *Hydrology and Earth System Sciences* **13** (2), 259–271. https://doi.org/10.5194/hess-13-259-2009.

Pells, S. E. & Pells, P. J. N. 2016 Application of Dupuit's equation in SWMM to simulate baseflow. *Journal of Hydrologic Engineering* **21** (1), 06015009. https://doi.org/10.1061/(ASCE)HE.1943-5584.0001245.

Peng, Z. & Stovin, V. 2017 Independent validation of the SWMM green roof module. *Journal of Hydrologic Engineering* **22** (9), 04017037. https://doi.org/10.1061/(ASCE)HE.1943-5584.0001558.

Peng, J., Zhong, X., Yu, L. & Wang, Q. 2020 Simulating rainfall runoff and assessing low impact development (LID) facilities in sponge airport. *Water Science and Technology* **82** (5), 918–926. https://doi.org/10.2166/wst.2020.400.

Puy, A., Piano, S. L., Saltelli, A. & Levin, S. A. 2022 **Sensobol**: An *R* package to compute variance-based sensitivity indices. *Journal of Statistical Software* **102** (5). https://doi.org/10.18637/jss.v102.i05.

Rosa, D. J., Clausen, J. C. & Dietz, M. E. 2015 Calibration and verification of SWMM for low impact development. *JAWRA Journal of the American Water Resources Association* **51** (3), 746–757. https://doi.org/10.1111/jawr.12272.

Rossman, L. A. 2010 *Storm Water Management Model User's Manual, Version 5.0*. National Risk Management Research Laboratory, Office of Research and Development, US Environmental Protection Agency.

Rossman, L. A. 2016 *Storm Water Management Model Reference Manual Volume I – Hydrology (Revised)*. National Risk Management Laboratory Office of Research and Development U.S. Environmental Protection Agency.

Rujner, H., Leonhardt, G., Marsalek, J., Perttu, A.-M. & Viklander, M. 2018 The effects of initial soil moisture conditions on swale flow hydrographs. *Hydrological Processes* **32** (5), 644–654. https://doi.org/10.1002/hyp.11446.

Saavedra, D., Mendoza, P. A., Addor, N., Llauca, H. & Vargas, X. 2022 A multi-objective approach to select hydrological models and constrain structural uncertainties for climate impact assessments. *Hydrological Processes* **36** (1). https://doi.org/10.1002/hyp.14446.

Sañudo-Fontaneda, L. A., Roces-García, J., Coupe, S. J., Barrios-Crespo, E., Rey-Mahía, C., Álvarez-Rabanal, F. P. & Lashford, C. 2020 Descriptive analysis of the performance of a vegetated swale through long-term hydrological monitoring: A case study from Coventry, UK. *Water* **12** (10), 2781. https://doi.org/10.3390/w12102781.

Seibert, J. 2000 Multi-criteria calibration of a conceptual runoff model using a genetic algorithm. *Hydrology and Earth System Sciences* **4** (2), 215–224. https://doi.org/10.5194/hess-4-215-2000.

Skougaard Kaspersen, P., Høegh Ravn, N., Arnbjerg-Nielsen, K., Madsen, H. & Drews, M. 2017 Comparison of the impacts of urban development and climate change on exposing European cities to pluvial flooding. *Hydrology and Earth System Sciences* **21** (8), 4131–4147. https://doi.org/10.5194/hess-21-4131-2017.

Sobol, I. M. 2001 Global sensitivity indices for nonlinear mathematical models and their Monte Carlo estimates. *Mathematics and Computers in Simulation* **55** (1–3), 271–280. https://doi.org/10.1016/S0378-4754(00)00270-6.

Storn, R. & Price, K. 1997 Differential evolution – A simple and efficient heuristic for global optimization over continuous spaces. *Journal of Global Optimization* **11** (4), 341–359. https://doi.org/10.1023/A:1008202821328.

Wu, Y., Jiang, Y., Yuan, D. & Li, L. 2008 Modeling hydrological responses of karst spring to storm events: Example of the Shuifang spring (Jinfo Mt., Chongqing, China). *Environmental Geology* **55** (7), 1545–1553. https://doi.org/10.1007/s00254-007-1105-z.

Xie, J., Wu, C., Li, H. & Chen, G. 2017 Study on storm-water management of grassed swales and permeable pavement based on SWMM. *Water* **9** (11), 840. https://doi.org/10.3390/w9110840.

Yang, W.-Y., Li, D., Sun, T. & Ni, G.-H. 2015 Saturation-excess and infiltration-excess runoff on green roofs. *Ecological Engineering* **74**, 327–336. https://doi.org/10.1016/j.ecoleng.2014.10.023.

First received 28 September 2023; accepted in revised form 23 November 2023. Available online 2 December 2023